Metrol. Meas. Syst., Vol. XVII (2010), No. 3, pp. 00–00

PAN POLSKA AKADEMIA NAUK

METROLOGY AND MEASUREMENT SYSTEMS

Index 330930, ISSN 0860-8229

www.metrology.pg.gda.pl

M&MS

INDOOR POSITIONING BY ULTRAWIDE BAND RADIO AIDED INERTIAL NAVIGATION

Alessio De Angelis[1)], John Olof Nilsson[1)], Isaac Skog[1)], Peter Händel[1)], Paolo Carbone[2)]

1) Royal Institute of Technology, Signal Processing Lab, ACCESS Linnaeus Centre, Osquldas väg 10, 10044 Stockholm, Sweden (✉ alessio.deangelis@ee.kth.se, +46 8 790 8435, jnil02@kth.se, isaac.skog@ee.kth.se, peter.handel@ee.kth.se)

2) University of Perugia, Department of Electronic and Information Engineering, Via G. Duranti 93, 06125 Perugia, Italy (carbone@diei.unipg.it)

Abstract

A research study aimed at developing a novel indoor positioning system is presented. The realized system prototype uses sensor fusion techniques to combine information from two sources: an in-house developed local Ultra-Wideband (UWB) radio-based ranging system and an inertial navigation system (INS). The UWB system measures the distance between two transceivers by recording the round-trip-time (RTT) of UWB radio pulses. Its principle of operation is briefly described, together with the main design features. Furthermore, the main characteristics of the INS and of the Extended Kalman Filter information fusion approach are presented. Finally, selected static and dynamic test scenario experimental results are provided. In particular, the advantages of the proposed information fusion approach are further investigated by means of a high dynamic test scenario.

Keywords: Ultra-Wideband, indoor positioning, inertial navigation.

1. Introduction

1.1. Indoor Positioning

The services based on communication networks are constantly advancing and are being used on a larger scale. As a result, the research of sensor networks has recently generated considerable interest. In particular, networks with mobile nodes constitute a challenging field, where research activities are focused on methods and systems for efficient and reliable information sharing and processing. User geographical location is a fundamental service that can be provided by a communication network. In outdoor applications, global navigation satellite systems (GNSSs) are commonly used, providing reliable position accuracy in the order of 3 to 10 m, sufficient for many applications. However, GNSSs typically perform poorly in indoor environments due to the signal attenuation and reflection introduced by buildings, walls and other structures. Nevertheless, there are many applications in which accurate indoor position information may be critical or, at least, improve efficiency. Some of these include safety-of-life operations, patient monitoring, industrial automation and warehouse management. Such applications often require high position accuracy, mainly due to the nature of the environment. An accuracy of about 1 m is typically sufficient to provide indications of the floor and room the user is in, but in some cases even higher accuracy is required. On the other hand, the operational area of application of an indoor positioning system is typically smaller and more controlled in comparison with that of an outdoor application. These features make it possible to install a positioning infrastructure and perform a preliminary calibration procedure during the system deployment phase.

Article history: received on Jun. 30, 2010; accepted on Aug. 31, 2010; available online on Sept. 6, 2010.

Many different approaches to solving the indoor positioning and navigation issues may be found in the scientific literature [1]. Some are built on a pre-existing communication infrastructure, such as a Wireless Local Area Network (WLAN) [2] or a ZigBee [3] sensor network, whilst other solutions are designed specifically for the main purpose of indoor positioning. The main advantage of using a pre-existing wireless communication infrastructure is the low cost, coupled with the benefit of the availability of a robust and standardized communication channel that may also be used to support the positioning system. The main drawback is often limited achievable accuracy, due to the fact that the systems are typically not designed for positioning. On the other hand, developing a system primarily aimed at positioning may require time and resources, but provides better control on specifications like accuracy, coverage and power consumption.

1.2. Ultra Wide Band Systems

In the context of indoor radio positioning, pulse-based Ultra-Wideband (UWB) is a technology of interest, mainly due to its fine temporal resolution and its resilience to multipath signal propagation [1, 4, 5]. According to the widely accepted definition, provided by the Federal Communications Commission Regulation [6], an UWB system is defined as any intentional radiator having a fractional bandwidth greater than 20% or an absolute bandwidth greater than 500 MHz. Such a wide spectral content may be obtained by generating pulses with transition times smaller than 1 ns. In the pulse-UWB positioning literature, examples of experimental systems design and characterization research activities can be found; having differences in scope, methods and applications [5, 7, 8]. Furthermore, there is a relatively small number of proprietary UWB ranging solutions; mainly intended for industrial, security or logistics indoor applications [9–11]. The performance specifications of these systems are an indoor accuracy of 10–50 cm and a maximum operating range in the order of 10–100 m.

1.3. Inertial Navigation Systems and Sensor Fusion for Positioning

An Inertial Navigation System (INS) adds attitude information to the positioning system that might be critical in some applications, making it possible to compensate for directional dependent disturbances. Furthermore, it increases the dynamic range of the combined system and can also eliminate shadow areas − where less than three UWB nodes are visible − by tracking the position for a limited period of time without the need for external measurement.

However, introducing the INS to the system adds the requirement of fusing its output with the information of the UWB ranging system. In the field of information fusion for indoor positioning, several approaches exist; involving the integration of different information sources, such as GPS, INS and local radio technologies. The most widely studied techniques are based on Extended Kalman filtering or non-linear filtering approaches such as Monte Carlo methods [12–14].

1.4. Scope

This paper presents a research study aimed at realizing a complete and scalable indoor navigation system. The system architecture is based on the combination of local radio infrastructure and inertial navigation. During this study, we have developed an in-house UWB ranging system that supports an INS. By implementing sensor fusion techniques, the system provides information about the position, velocity and attitude of a mobile node. Some of the results obtained from experimentation using the system have been previously presented in

[15] and in [16], including a description of the main system characteristics from a system-level point of view. Furthermore, an in-depth discussion on the signal processing techniques used and the related issues have been presented in [17].

1.5. Outline

The outline of the paper is as follows. In Section 2, a system overview is presented and the main features of the UWB radio positioning subsystem and the INS are outlined. Thereafter, in Section 3, the sensor fusion of the information provided by the two sources is discussed. In Section 4, the experimental setup used to test the system and the test results are presented. Finally, in Section 5, conclusions regarding the work are drawn.

2. System overview

The indoor navigation system consists of the infrastructure segment and the user segment. It is schematically presented in Fig. 1.

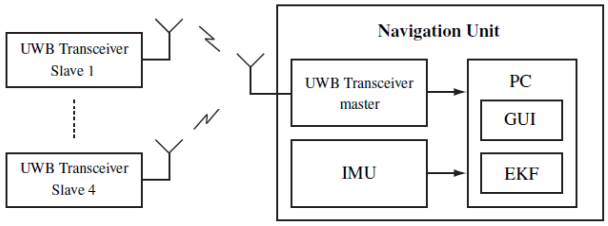

Fig. 1. Functional diagram of the complete indoor positioning system [15].

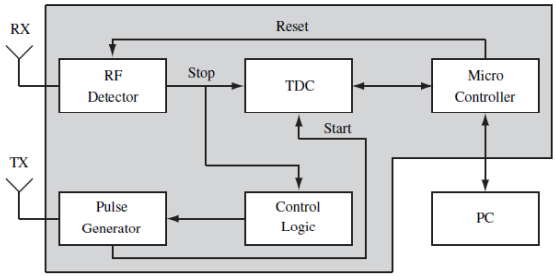

Fig. 2. Architecture of the UWB master device [15].

The infrastructure segment comprises a set of UWB radio nodes located at known positions within the operational area. The user segment is the navigation unit, which aims to estimate its location and attitude relative to the UWB radio nodes by combining UWB radio range measurements and inertial navigation. To achieve this task, the navigation unit comprises:

- An UWB ranging device (master unit, see Section 2.1) measuring the ranges to UWB radio nodes (slave units, see Section 2.1).
- An inertial measurement unit (IMU) providing acceleration and angular rate measurements for the INS.
- A PC running the mechanization equations of the INS and an extended Kalman filter (EKF); where the EKF is used to combine the information from the INS with the measurements of the UWB ranging system, yielding a joint navigation solution.

2.1. Ultra wide band radio distance measurements

The principle of operation of the UWB ranging system is based on the indirect measurement of the distance between transceivers, obtained by measuring the round-trip time (RTT) of an UWB pulse [5]. This approach does not require temporal synchronization, which is an advantage when compared to other commonly used strategies such as time-of-arrival or time-difference-of-arrival [1, 4]. However, when measuring the RTT, the latency introduced by the responder devices has to be accurately measured or estimated. In the present system, this issue is addressed by performing a calibration of each slave unit [15, 18].

The system is comprised of a master device and several slaves. The master transceiver is capable of measuring RTT. This time interval measuring function is performed by a commercial time-to-digital converter (TDC) integrated circuit, the TDC-GP2 by Acam Messelectronic GmbH, with a root-mean-square (RMS) resolution of 50 ps. A block diagram of the master is shown in Fig. 2. The slave devices are not designed to perform time interval measurements; but will instead − on request after a fixed delay − echo a UWB pulse with another UWB pulse, thus providing a "round trip". The slave unit has two modes of operation: communication mode and responder mode. Fig. 3a shows a functional block diagram of the devices in communication mode, whilst the responder mode is illustrated in Fig. 3b. Using logic circuits, the slave devices switch between the two modes of operation. The circuit architectures of both the master and the slave devices are based on the system presented in [19], whilst the UWB pulse generator modules have been built using step recovery diodes using the circuit design presented in [20].

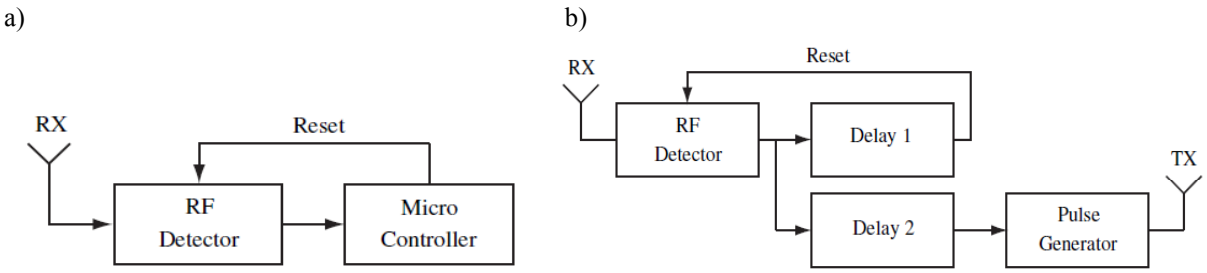

Fig. 3. Simplified architecture of the slaves in the two operating modes: a) communication mode; b) responder mode [15].

Furthermore, omnidirectional wideband disc-cone antennae have been used in the receiving and transmitting sections of each device. Fig. 4 shows a picture of one of the realized prototypes.

Fig. 4. Picture of the realized prototype of the master device [15].

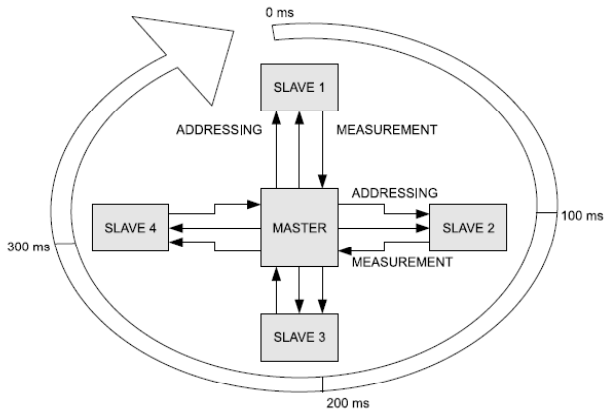

Fig. 5. Operation of the system, showing the addressing and measurement phases, together with timing information [15].

An example of timing diagram for the operation of the system is provided in Fig. 5. It is divided in two sequential phases − addressing and measurement. In the first phase, the master sends an 8-bit unique slave identifier code, using on-off keying with UWB pulses. In this basic modulation scheme, if a pulse is transmitted within a specific time slot, it is interpreted as a "1" bit. The absence of a pulse is seen as a "0" bit. During the addressing phase all the

slaves are in communication mode and receive this message. At the end of this phase only the slave corresponding to the unique identifier is activated and transitions to the responder state.

The other slaves are disabled for a fixed amount of time. Subsequently, during the measurement phase, the master sends ten measurement pulses and measures the RTT of each pulse. The measurement pulses are spaced approximately 5 ms apart. After each pulse, the measurement result is sent to the PC through a serial interface. This procedure is repeated every 100 ms; hence the system is able to obtain measurement sets (ten measurements) from slaves at a frequency of 10 Hz. The reason the measurements are done in groups of ten is that the addressing phase is relatively long (approximately 40 ms) in comparison with the time between the single measurements (approximately 5 ms).

Using only the UWB ranging system described above, with a tracking filter, it is possible to obtain position estimates relative to the infrastructure with a bounded error. However, this solution has a relatively low dynamic range. Furthermore, the system is sensitive to external radio disturbances that may cause integrity issues.

2.2. Inertial navigation

The INS can be divided into a sensor part (the IMU), and a computation part which in turn consist of a sensor model, a gravity model and mechanization equations. In our case the IMU is an Inertia Link® from MicroStrain®. The IMU contains a temperature compensated MEMS triaxial accelerometer and gyroscope. The computations are implemented on the PC to which the IMU is connected. An illustration of the INS can be seen in Fig. 6. Further details not presented below − derivations and descriptions of the INS − can be found in standard inertial navigation literature [21−25].

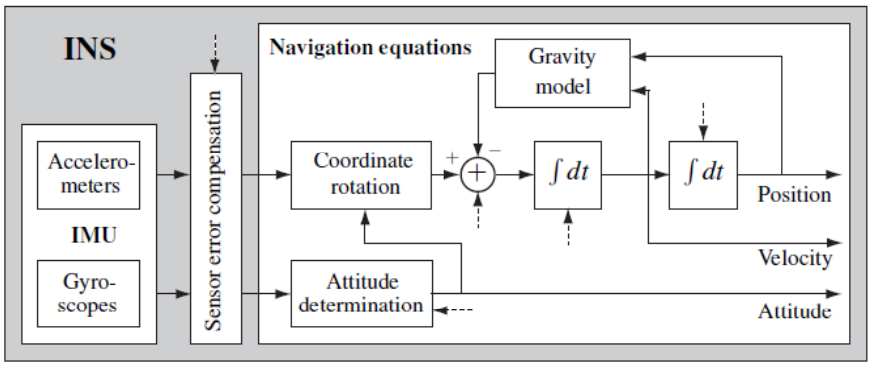

Fig. 6. Conceptual diagram of a strap-down INS. The dash arrows indicate points for insertion of calibration (aiding) data [27].

The sensor model relates the IMU output to the true specific force and angular rates (an ideal output) affecting the sensor elements:

$$\tilde{\mathbf{u}}_k = g(\mathbf{u}_k, \mathbf{b}_k) + \mathbf{n}_{1,k}, \tag{1}$$

where $\tilde{\mathbf{u}}_k$ is the IMU output, $g(\cdot)$ is the sensor model, u_k is the ideal output, k is a time index, $\mathbf{b}_k$ is the vector of sensor parameters, and $\mathbf{n}_{1,k}$ is a noise term. For the IMU sensor element type, in the current implementation and the dynamic range of the intended applications, the IMU output was modeled as the sum of the true values, a low-frequency noise component and a white noise term. For other IMU sensor element types and other dynamic ranges, the use of sensor models with higher or lower degrees of freedom might be desirable.

The gravity model is a model for the gravitational acceleration which will unavoidably enter into the accelerometer output. Due to the limited operational area of indoor applications and the signal to noise ratios of the IMU, a constant gravitational acceleration was used.

The INS mechanization equations describe the propagation of the navigational states $\mathbf{x}_k$ (position, velocity, and orientation in three dimensions) in time:

$$\mathbf{x}_{k+1} = f_{nav}(\mathbf{x}_k, \mathbf{u}_k) + \mathbf{n}_{2,k}. \tag{2}$$

Here the noise term $\mathbf{n}_{2,k}$ describes the deviation of the INS mechanization equations $f_{nav}(\cdot)$ from the ideal kinematic equations as well as the imperfections of the gravity model.

Given an initial estimate of the navigational states $\hat{\mathbf{x}}_\mathbf{o}$ and inertial measurements $\tilde{\mathbf{u}}_k$ for all k assuming the sensor model to be invertible in the range of the inertial measurements, and the estimates of the sensor model parameters $\hat{\mathbf{b}}_k$ given, the INS can, as a standalone system, give estimates of the navigational states for all k by propagating the estimates according to:

$$\hat{\mathbf{x}}_{k+1} = f_{ins}(\hat{\mathbf{x}}_k, g^{-1}(\tilde{\mathbf{u}}_k, \hat{\mathbf{b}}_k)). \tag{3}$$

Due to the intrinsic robustness and integrity of the inertial measurements, the typically high sampling rate of inertial sensors, and the fact that time derivatives of position and orientation are measured, high dynamic range and good performance for short time periods are achieved. Unfortunately, the propagation of the navigation equations essentially contains three integrations, one in the orientation propagation and two in the velocity and position propagation respectively. As a consequence, the sensor noise and model imperfections together with the constant input from gravity will cause errors in the estimates of (3) to compound approximately cubically with time. For the current INS implementation/IMU performance, this implies unacceptable errors (>1 m) after only a few seconds.

3. Information fusion

The objective of information fusion is to obtain more information than is present in any individual source by combining information from different sources [26]. As noted above, the INS has unbounded error growth but provides a self-contained and robust estimation of all the navigational states and is further capable of handling high dynamics. On the other hand, the UWB ranging system does not provide attitude information, has poor dynamic range and poor robustness to external disturbances, but has bounded errors. Combining these two systems compensates for the shortcomings of both and yields better performance than possible from any individual system. The complementary subsystem characteristics are summarized in Table 1.

Table 1. Summary of the complementary properties of the two information sources (UWB and INS).

	Navigational states	**Dynamic range**	**Stand-alone error**	**Self-contained (high-integrity)**
UWB	NO	LOW	**BOUNDED**	NO
INS	**YES**	**HIGH**	UNBOUNDED GROWTH	**YES**

The inertial navigation and the ranging have a nonlinear dependence on the navigation states, making the optimal information fusion difficult. Hence, some approximate techniques have to be employed [27]. To limit the system complexity and to facilitate implementation, a complementary filter structure − implemented with an extended Kalman filter (EKF) − was used. This results in a so called range-aided INS. A diagram of the filter structure is shown in Fig. 7. This structure allows full use of the complementary properties of the two information sources.

The complementary filter structure implies that the errors in the estimates of the underlying system states and parameters are estimated, rather than the states and parameters themselves. In particular, in the current system the errors in the estimates of the navigational states and of the sensor model parameters (errors in the INS) are estimated. Subsequently the errors estimates are fed back into the INS, allowing the linearization point of the EKF to be always kept at zero; that is, any non-zero error estimate is directly compensated for in the INS.

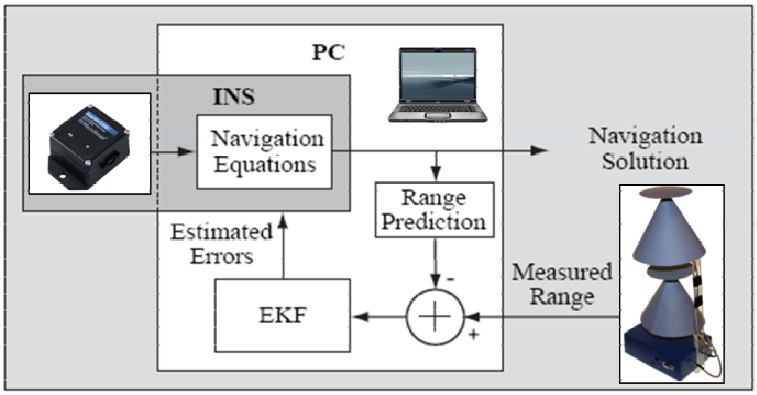

Fig. 7. Information fusion system architecture, based on the complementary filtering approach [15].

Defining the error $\delta\alpha_k$ in the estimate $\hat{\alpha}_k$ of the quantity α_k as:

$$\delta\alpha_k = \alpha_k - \hat{\alpha}_k$$

and assuming that the errors in the navigation state and sensor model parameters are small, the INS mechanization equations together with the sensor models are used to derive differential equations for the propagation of the errors as:

$$\left[\delta\mathbf{x}_{k+1}^T \;\; \delta\mathbf{b}_{k+1}^T\right]^T = f_{err}\left(\left[\delta\mathbf{x}_k^T \;\; \delta\mathbf{b}_k^T\right]^T, \tilde{\mathbf{u}}_k\right) + \mathbf{n}_{3,k}, \tag{4}$$

where the noise term $\mathbf{n}_{3,k}$ describes the combined effect of $\mathbf{n}_{1,k}$ and $\mathbf{n}_{2,k}$ and approximations (typically discarding higher order terms) made in the derivation of (4). The error model (4) is the fundamental process that the EKF will estimate. Derivation and descriptions of error models can be found in [23, 24].

The states of the EKF are the errors in navigation state and sensor model parameter estimate, as given by the INS. Therefore, to aid the INS with the range measurements $\tilde{z}_k$ of the UWB ranging system, these measurements have to be related to the same error states. Based on a known slave position $\mathbf{r}_{slave,k}$, to which the ranging is done at time instant k, and the navigational states estimate (subcomponent position denoted $\hat{\mathbf{r}}_k$), a range estimate $\hat{z}_k$ can be calculated. Assuming the error in the range measurement $\delta\tilde{z}_k$ to be zero-mean, this means that this range estimate can be seen as an estimate of both the true range and the measured

range. Then, as shown in [17], from the error in the range estimate and range measurement a measurement model:

$$\tilde{z}_k = h_k(\delta \mathbf{x}_k) + n_{4,k} \tag{5}$$

can be derived, where:

$$h_k(\delta \mathbf{x}_k) = \left|\mathbf{r}_{slave,k} - (\delta \mathbf{r}_k + \hat{\mathbf{r}}_k)\right| - \left|\mathbf{r}_{slave,k} - \hat{\mathbf{r}}_k\right|$$

and where $n_{4,k}$ is the error in the range measurement. Furthermore, a fact commonly neglected in the measurement equations is that the measurements $\tilde{z}_{l,k}$ and the driving input signal $\tilde{\mathbf{u}}_k$ are often neither synchronous (exist for the same k) nor appended with any perfect temporal information with respect to a common time reference. This is handled by a zero-order hold assumption and by estimating time stamps of the data as described in [28].

Given the relations (4) and (5) and the covariances of $\mathbf{n}_{3,k}$ and $n_{4,k}$, and by propagating (2), the EKF framework can be applied. Additionally, as noted above, any non-zero error estimate ought to be fed back to the INS. Hence, after the update phase of the EKF, the error estimates $\left[\delta\hat{\mathbf{x}}_k^T \quad \delta\hat{\mathbf{b}}_k^T\right]^T$ will be fed back to the navigation states estimates $\hat{\mathbf{x}}_k$ and the sensor model parameter estimates $\hat{\mathbf{b}}_k$ respectively. This will significantly simplify the EKF implementation as discussed in [17]. Details of the Kalman filter can be found in standard estimation literature, *e.g*. [29].

4. Test results

To calibrate and characterize the system, a series of measurements were conducted. The measurements were carried out in an indoor office environment under line-of-sight conditions.

4.1. UWB ranging calibration

The basic measurements in the UWB ranging system are the RTT of the UWB radio pulses. The RTT depends on the distance the pulse has to travel and the latency introduced by the hardware (hardware signal path, intentional delay buffers, detector rise-time, *etc*.) in the slave and master units. Primarily due to varying cabling length and pulse detector threshold settings, but also manufacturing tolerances of other components, this latency will vary slightly from one slave unit to the next. Hence, to properly convert the RTT measurements into range measurements, each UWB slave unit needs to be calibrated individually. Moreover, for a proper information fusion in the EKF, the measurement error variances of the range measurements − as a function of the true distances − should be estimated from the calibration procedure.

The calibration was done by placing the slaves at manually measured (reference) distances from the master; at each distance 1000 RTT values were recorded. The resulting mean RTT values as a function of distance are shown in Fig. 8a, whilst the standard deviation values are shown in Fig. 8b.

A linear fit was performed on the RTT measurements and subsequently used to transform the RTT measurements to range measurements. For the measurement error variance, an exponential function was fitted to the standard deviation of the RTT measurements. By scaling by the reciprocal of the slope of the linear fit of the RTT measurements, and by squaring, the relation was converted into variance of the range measurements.

a) b)

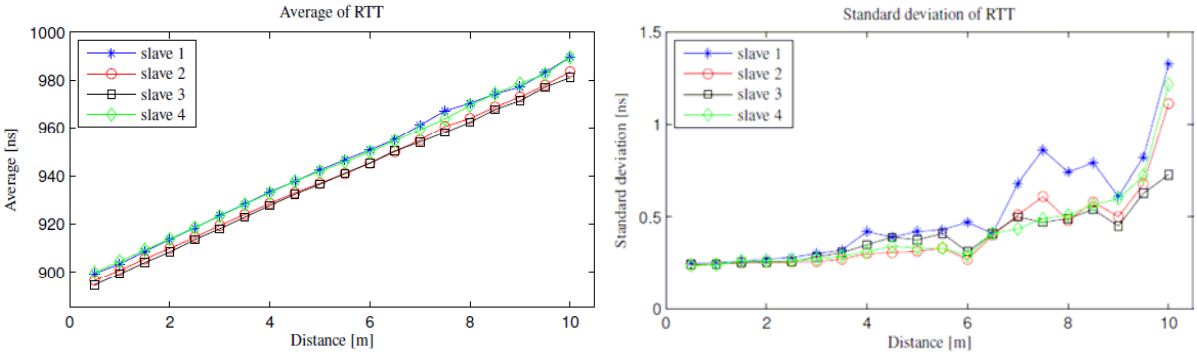

Fig. 8. Results from the calibration phase of the UWB system: Calibration curves used to convert the observed RTT into distance estimates [15].

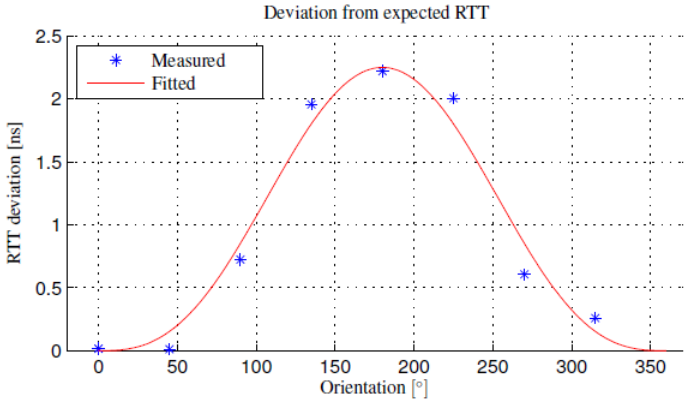

Fig. 9. Calibration results used to compensate for the orientation-dependent disturbances [15].

Further, due to self-interference from antenna cables and antenna stand, the RTT showed a directional dependence. The effect of this dependence was measured by placing a slave unit at a fixed distance while turning the master. At each turning point 1000 RTT measurements were taken and the expected RTT based on the RTT-to-range calibration was subtracted. The resulting deviation can be seen in Fig. 9. A sinusoidal function was fitted to the data and subsequently used to compensate for the directional dependence.

4.2. UWB only positioning

The UWB range measurements may be used to provide a position estimate as a stand-alone system; however, in this case they have the limitations mentioned in Section 2. To assess the characteristics of the range measurements and their stand-alone positioning performance, the following experiments were conducted.

– A static test scenario: The four UWB slave units were located in the corners of a 3x3-meters square and 5000 measurements cycles (*i.e.* distance measurement to all four slaves) for each unit were collected for the master placed in the centre (1.50 m, 1.50 m) and for the master placed off-centre (1.00 m, 1.00 m), such that the distance-dependent covariance would become observable. For each cycle the position of the master was calculated as a least squares solution giving a position estimate distribution. In Fig. 10 scatter plots together with 68% confidence regions and histograms of the position estimates are shown.

a) b)

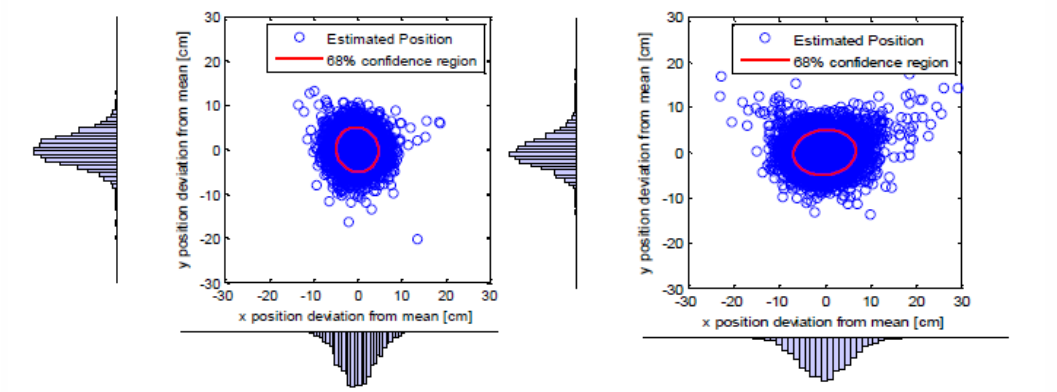

Fig. 10.Static measurement tests results, in two different positions: a) centre of the square test area (position = 1.5 m, 1.5 m), providing the best geometrical configuration possible; b) an off-centre position (1 m, 1 m) where a larger spread of the estimated positions is noticeable.

– A low dynamic test scenario: The four UWB slave units were located in the corners of a rectangle and the UWB master unit was slowly (approximate speed 0.1 m/s) moved in a 1x1 meter square trajectory. The master was held in a constant orientation to enable the correction of the orientation dependence of the RTT. Modeling the acceleration of the UWB master unit as random walk, a real-time tracking filter (an EKF) was implemented. The resulting estimated positions can be seen in Fig. 11a.

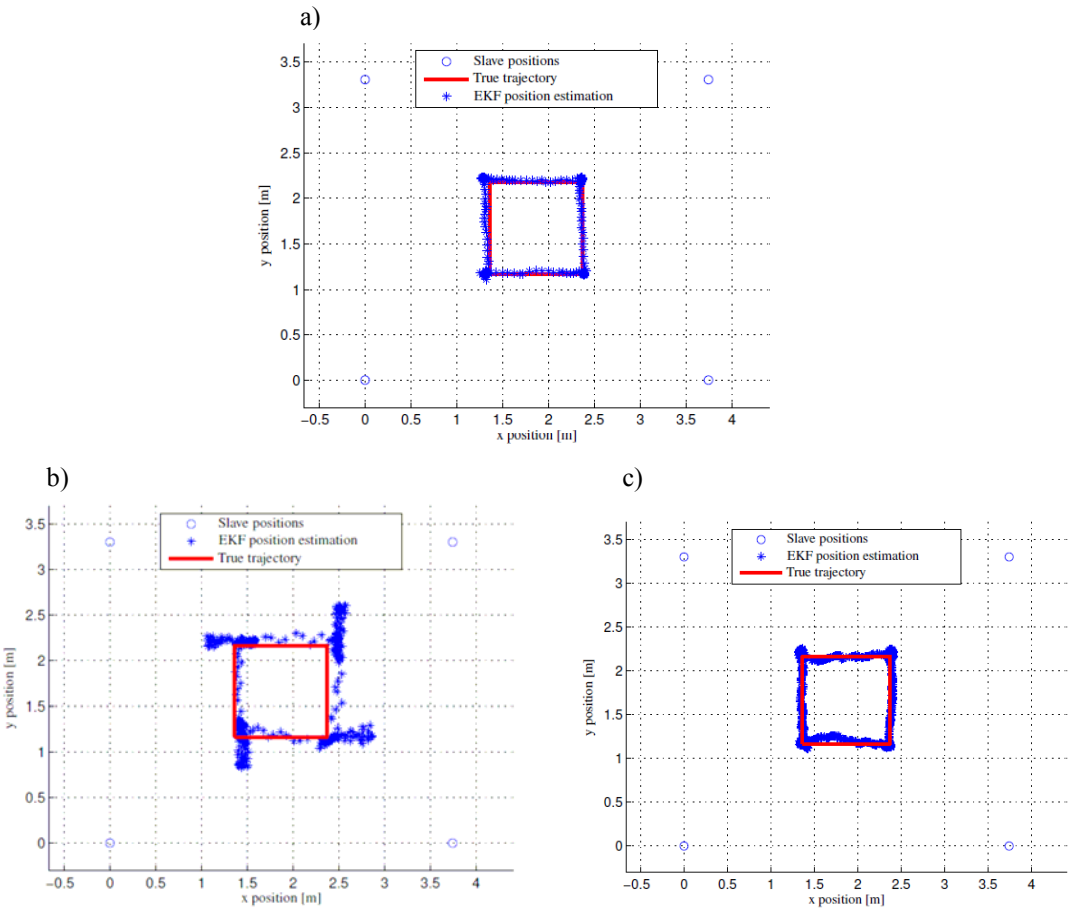

Fig. 11. Dynamic tests results. the master was moved along a square trajectory, shown in red. Three measurement scenarios are presented: a) low dynamic UWB-only, with an approximate speed of 0.1 m/s; b) high dynamic UWB-only with a speed of the order of magnitude of 1 m/s; c) high-dynamic with UWB/INS fusion, calculated using the same data as b) [15].

The position estimate is seen to provide good accuracy in this low dynamic scenario. The slow motion is tracked smoothly and the noise compared to the static scenario (least-squares solution) is suppressed by the tracking filter. Note that as the range measurements are asynchronous, the least-squares solution cannot be used in a non-static test scenario. Hence, some assumptions have to be made about the dynamics, as done in the driving noise covariance of the tracking filter.

– A high dynamic test scenario: Measurements were also done with the same trajectory, slave constellation, and tracking filter as in the low dynamic test scenario but with the master jerked from corner to corner as fast as possible. The resulting estimated position can be seen in Fig. 11b. To enable a comparison with the combined UWB and INS positioning, no directional correction was done. As a result, systematic errors can clearly be seen. Furthermore, in comparison with the low dynamic test scenario, the limited dynamic range can be observed in the overshoots in the corners and in the jagged estimated trajectory. The high dynamic test scenario is intended as an illustration of the limitations of the position estimate based on range measurement only. Hence, no attempts of optimizing the trade-off between noise suppression and dynamic range (overshoots) with respect to average position error have been made. It is however recognized that there is a fundamental deficiency in information obtained for high dynamic maneuvers tracked by the UWB range measurements only.

4.3. Combined INS and UWB positioning

The poor performance in the high dynamic test scenario of the UWB-only positioning is due to the limited dynamic range of the UWB system and the lack of orientation information. The INS, on the other hand, provides a high dynamic range as well as orientation information. Combining the INS and the UWB will give a high dynamic range and the ability to correct for the orientation dependence of the RTT, thus removing the systematic errors in the high dynamic test scenario of the UWB-only positioning. However, the INS based on MEMS inertial sensors typically only provides relative orientation information in the yaw direction. Fortunately the yaw orientation estimates of the INS are coupled with the position and velocity estimates, which in turn can be coupled to the UWB range measurements via (5). However, for the coupling between yaw orientation estimates and position and velocity estimates to arise, there needs to be a change in position and velocity in the yaw plane, that is horizontal accelerations.

In Fig. 11c the same trajectory as that of the high dynamic test scenario of the UWB-only positioning is shown, but with the inertial navigation and sensor fusion applied. In Fig. 12, the results of another data set are shown, comprising two laps along the same square trajectory (Fig. 12a and 12b). Clearly the effects of the limited dynamic range (overshoots at the corners and the jagged lines), as well as the systematic errors due to the directional dependence of the UWB range measurements, have been removed. The resulting orientation estimate, for both laps and an initial stationary phase, is shown in Fig. 12c. The initial jump to 20° is a mere filter artifact and the associated orientation state estimation error covariance is large. The initial INS state vector $\boldsymbol{x}_0$, as well as the error state vector $\delta\boldsymbol{x}_0$, were both initialized to zero, whilst the estimation error covariances were initialized to large values. The position, as well as the roll and pitch, converge swiftly during the initial stationary phase whilst the yaw starts to converge as soon as there is acceleration in the horizontal plane, and reaches a steady orientation estimate during the second lap. The erroneous orientation estimates during the first lap can clearly be seen, especially along the first (lower) side of the trajectory of Fig. 12a. This behavior disappears around the second lap, for which the orientation has converged. The position discrepancy for the second lap between the estimated and the manually measured

trajectory is below 4 cm. However, due to difficulties of measuring the exact position of the antennae and the system in motion, the uncertainty of the true trajectory is estimated to be of the same order of magnitude. The same holds for the true orientation; however the correct behavior of the position estimates around the second lap, as in contrast to the first lap, indicates that approximately the right yaw has been estimated.

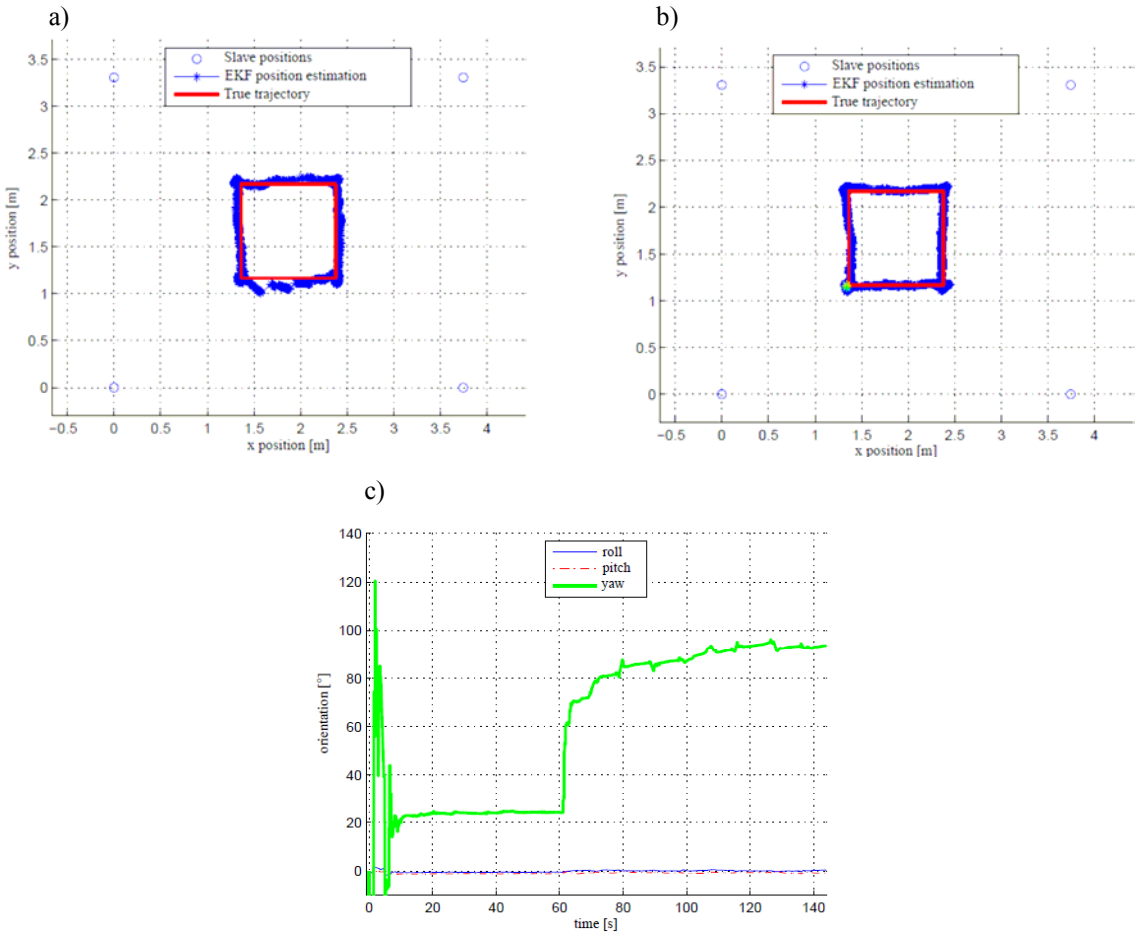

Fig. 12. Results from a test on the sensor fusion system, 2-laps square trajectory. a) First lap. b) Second lap. c) Orientation estimate vs. time (roll, pitch and yaw angles), the first lap starts at approximately 60 s, and the second at approximately 100 s [17].

5. Conclusion

In this paper, an indoor positioning system has been introduced by describing its architecture and presenting some experimental results. The system is based on the integration between an UWB positioning system and an INS. Particular focus has been given to the description of the system components and their principle of operation. The experimental test results have shown the system capability to statically and dynamically measure the position with accuracy of the order of 5 centimeters in a controlled indoor environment. Combining INS and UWB positioning provides a higher dynamic range and improved performance than possible with any of the individual systems. As an additional benefit, the orientation estimate is also provided by the system.

References

[1] H. Liu, H. Darabi, P. Banerjee, and J. Liu: "Survey of wireless indoor positioning techniques and systems". *IEEE Trans. Syst., Man, Cybern. C, Appl. Rev.*, vol. 37, Nov. 2007, pp. 1067–1080.

[2] IEEE Std 802.11-2007, *Standard for Information Technology-Telecommunications and Information Exchange Between Systems-Local and Metropolitan Area Networks-Part 11,* 2007.

[3] ZigBee Alliance. 2009, *http://www.zigbee.org/*

[4] S. Gezici *et al*.: "Localization via ultra-wideband radios: a look at positioning aspects for future sensor networks". *IEEE Signal Processing Magazine*, vol. 22, Jul. 2005, pp. 70–84.

[5] R. Fontana: "Recent system applications of short-pulse ultrawideband (UWB) technology." *IEEE Trans. Microw. Theory Tech.*, vol. 52, Sep. 2004, pp. 2087–2104.

[6] *Federal Communications Commission (FCC). Revision of part 15 of the commission's rules regarding ultra-wideband transmission systems*, 2002.

[7] L. Stoica, A. Rabbachin, H.O. Repo, T.S. Tiuraniemi, I. Oppermann: "An ultrawideband system architecture for tag based wireless sensor networks". *IEEE Trans. Vehic. Techn.*, vol. 54, Sep. 2005, pp. 1632–1645.

[8] M.R. Mahfouz, C. Zhang, B.C. Merkl, M.J. Kuhn, A.E. Fathy: "Investigation of high-accuracy indoor 3-D positioning using UWB technology." *IEEE Trans. Microw. Theory Tech.*, vol. 56, Jun. 2008, pp. 1316–1330.

[9] *Multispectral Solutions, Zebra Enterprise Solutions*. Jun. 2010, Sapphire DART (RTLS) product data sheet. *http://zes.zebra.com/pdf/products-datasheets/ds_sapp_dart.pdf*

[10] *Time Domain Corporation*. Jun. 2010, PulsON P220 reference Design. *http://www.timedomain.com/products/P220aRD.pdf*

[11] *The Ubisense Precise Real-time Location System*. Ubisense Ltd. Jun.2010, *http://www.ubisense.net*

[12] J. Gonzalez *et al*.: "Combination of UWB and GPS for indoor-outdoor vehicle localization". *Proc. IEEE International Symposium on Intelligent Signal Processing, WISP*, Alcala de Henares, Spain, 3–5 Oct. 2007.

[13] K.M. Tan, C.L. Law: "GPS and UWB integration for indoor positioning". *Proc. 6th International Conference on Information, Communications & Signal Processing*, Singapore, 10–13 Dec. 2007.

[14] D.B. Jourdan, J. Deyst, M.Z. Win, N. Roy: "Monte Carlo localization in dense multipath environments using UWB ranging". *Proc. IEEE International Conference on Ultra-Wideband ICUWB*, Zurich, Switzerland, 5–8 Sept. 2005, pp. 314–319.

[15] A. De Angelis, J.O. Nilsson, I. Skog, P. Händel, P. Carbone: "Indoor positioning by ultra wideband radio aided inertial navigation". *XIX IMEKO World Congress*, Lisbon, Portugal, Sept. 2009, pp. 574–579.

[16] De Angelis, A. Moschitta, P. Händel, P. Carbone: "Experimental radio indoor positioning systems based on round-trip-time measurement". *Advances in Measurement Systems,* chapter 8*,* ed. Milind Kr Sharma, INTECH, 2010.

[17] J.O. Nilsson, A. De Angelis, I. Skog, P. Carbone: "Signal processing issues in indoor positioning by ultra wide band radio aided inertial navigation". *European Signal Processing Conference Proceedings, EUSIPCO*, Glasgow, Scotland, August 2009, pp. 2161–2165.

[18] A. De Angelis, M. Dionigi, A. Moschitta, P. Carbone: "A low-cost ultra-wideband indoor ranging system". *IEEE Trans. Instrum. Meas.*, vol. 58, no. 12, Dec. 2009, pp. 3935–3942.

[19] A. De Angelis, M. Dionigi, A. Moschitta, R. Giglietti, P. Carbone: "Characterization and modeling of an experimental UWB pulse-based distance measurement system". *IEEE Trans. Instrum. Meas.*, vol. 58, no. 5, May 2009, pp. 14791–1486.

[20] M. Dionigi, R. Giglietti, P. Carbone A. De Angelis: "Experimental low-cost short pulse generators". *IEEE Instrum. and Meas.Techn. Conference Proceedings, IMTC*, Victoria, BC, Canada, 2008, pp. 259–264.

[21] K.R. Britting: *Inertial Navigation Systems Analysis*. Wiley Interscience, 1971.

[22] C. Jekeli: *Inertial Navigation Systems with Geodetic Applications*. de Gruyter, 2001.

[23] J. Farrell, M. Barth: *The Global Positioning System & Inertial Navigation*. McGraw-Hill, 1999.

[24] A. Chatfield: *Fundamentals of High Accuracy Inertial Navigation*. American Institute of Aeronautics and Astronautics, 1997.

[25] M.S. Grewal, L.R. Weill, A.P. Andrews: *Global Positioning Systems, Inertial Navigation and Integration*. Wiley, 2007.

[26] L. Yan, B. Liu, D. Zhou: "Asynchronous multirate multisensor information fusion algorithm". *IEEE Trans. Aero. Elec. Sys.*, vol. 43, July 2007, pp. 1135–1146.

[27] I. Skog, P. Händel: "In-car positioning and navigation technologies – a survey". *IEEE Trans. Intell. Tran. Syst.*, vol. 10, no. 1, Mar. 2009, pp. 4–21.

[28] J.O. Nilsson, P. Händel: "Time synchronization and temporal ordering of asynchronous measurements form a multi-sensor navigation system". *IEEE/ION Position Location and Navigation System (PLANS)*, Palm Springs, USA, May 2010.

[29] T. Kailath, A. Sayed, B. Hassibi: *Linear Estimation*. Prentice-Hall, 2000.